Journal of Alloys and Compounds 509 (2011) 7814–7818

Contents lists available at ScienceDirect

Journal of Alloys and Compounds

journal homepage: www.elsevier.com/locate/jallcom

Cascade structure of TiO_2/ZnO/CdS film for quantum dot sensitized solar cells

Guang Zhu[a], Likun Pan[a,*], Tao Xu[a], Qingfei Zhao[b], Zhuo Sun[a]

[a] Engineering Research Center for Nanophotonics & Advanced Instrument, Ministry of Education, Department of Physics, East China Normal University, Shanghai 200062, China
[b] Chemistry Department, Shanghai Normal University, Shanghai 200234, China

ARTICLE INFO

Article history:
Received 8 April 2011
Received in revised form 10 May 2011
Accepted 12 May 2011
Available online 19 May 2011

Keywords:
ZnO film
CdS
Quantum dot sensitized solar cell
Ultrasonic spray pyrolysis

ABSTRACT

Quantum dot sensitized solar cells based on cascade structure of TiO_2/ZnO/CdS electrode and polysulfide electrolyte were fabricated. The ZnO layer was deposited on screen-printed TiO_2 layer by ultrasonic spray pyrolysis method. The structure, morphology and impedance of TiO_2/ZnO film photoanode and the photovoltaic performance of TiO_2/ZnO/CdS cell were investigated. It is found that the short circuit current density and conversion efficiency are significantly improved by the introduction of ZnO layer into TiO_2/CdS film. A power conversion efficiency of about 1.56% has been obtained for TiO_2/ZnO/CdS cell, which is about 57% higher than that for TiO_2/CdS cell (0.99%). The formation of an inherent energy barrier between TiO_2 and CdS films and the passivation of surface traps on the TiO_2 film caused by the introduction of ZnO layer, which reduces the charge recombination and favors the electron transport, should be mainly responsible for the performance enhancement of TiO_2/ZnO/CdS cell.

1. Introduction

Sensitized solar cells (SSCs) have attracted considerable attention and represent a key class of cell architecture that has emerged as a promising candidate for the development of next generation solar cells due to their acceptable power conversion efficiency and low production cost [1–16]. SSCs are based on the photosensitization of nanocrystalline TiO_2 or ZnO semiconductor photoanode by absorbed dye or quantum dot (QD) sensitizers. As a key component of SSCs, the structure, size, characteristics of photoanode have been studied to improve SSC efficiency [17–24,8]. Many studies have also devoted to explore more sophisticated structures to optimize the performance of photoanode. For example, TiO_2 film is coated with wide band gap ZnO layer to form an inherent energy barrier and suppress the charge recombination at the interface of the electrode/electrolyte. Wang et al. [25] reported dye SSCs (DSSCs) with a conversion efficiency of 2.15% based on ZnO-nanowire-covered TiO_2 nanoparticle composite film electrodes which were fabricated by low-temperature hydrothermal growth of ZnO nanowries on screen-printed TiO_2 nanoparticle layer. Roh et al. [26] reported the use of ZnO recombination barrier layer by successive ionic layer adsorption and reaction (SILAR) method on TiO_2 layer to improve the efficiency of DSSCs by 36% from 3.31% to 4.51%. Wu et al. [27] fabricated ZnO-coated TiO_2 electrode by rf magnetron sputtering to increase the efficiency of DSSCs by 38% from 4.76% to 6.55%. Kao et al. [28] studied DSSCs based on ZnO-coated TiO_2 film fabricated by sol–gel method and found that the conversion efficiency was increased to 3.24% as compared with 2.5% for DSSC based on bare TiO_2 film. Kim et al. [29] prepared TiO_2/ZnO/Eosin Y films by one-step cathodic electrodeposition method for photoanode of DSSCs and found that the efficiency was increased from 2.6% for the cell without ZnO interlayer to 4.4%. Kim et al. [30] used ZnO-covered TiO_2 obtained by thermal chemical vapor deposition as photoanode of DSSCs and the efficiency was enhanced by 23% from 3.5% to 4.3% due to the passivation of surface traps on the TiO_2 film by ZnO coating. Kang et al. [31] fabricated TiO_2 nanotubes coated with an approximately 1 nm ZnO shell by electrochemical method for solid-state DSSCs and found that the thin ZnO coating enhanced the conversion efficiency from 0.578% for bare TiO_2 electrode to 0.704% by passivating the recombination centers on TiO_2 surface and reducing charge recombination. Wang et al. [32] used ZnO-covered TiO_2 nanoporous electrode for DSSCs and found that the efficiency was enhanced by 27.3% due to a positive shift of flat band potential and an increase in free electron concentration in the conduction band with respect to pure TiO_2 electrode. Lee et al. [33] fabricated TiO_2 nanotubes coated with a thin ZnO layer by SILAR method and studied the performance of CdSe QD SSCs (QDSSCs) based on such electrodes. It was found that the thin ZnO coating enhanced the conversion efficiency of the CdSe QDSSCs by 26% from 0.85% for bare TiO_2 electrode to 1.07%. They ascribed the improvement in the performance of cells to the enhancement of charge-collection efficiency and the hindrance of charge recombination by coating a thin ZnO energy barrier layer.

* Corresponding author at: Department of Physics, Engineering Research Center for Nanophotonics & Advanced Instrument, East China Normal University, 3663 North Zhongshan Road, Shanghai 200062, China. Tel.: +86 21 62234132; fax: +86 21 62234321.
E-mail address: lkpan@phy.ecnu.edu.cn (L. Pan).

0925-8388/$ – see front matter © 2011 Elsevier B.V. All rights reserved.
doi:10.1016/j.jallcom.2011.05.043

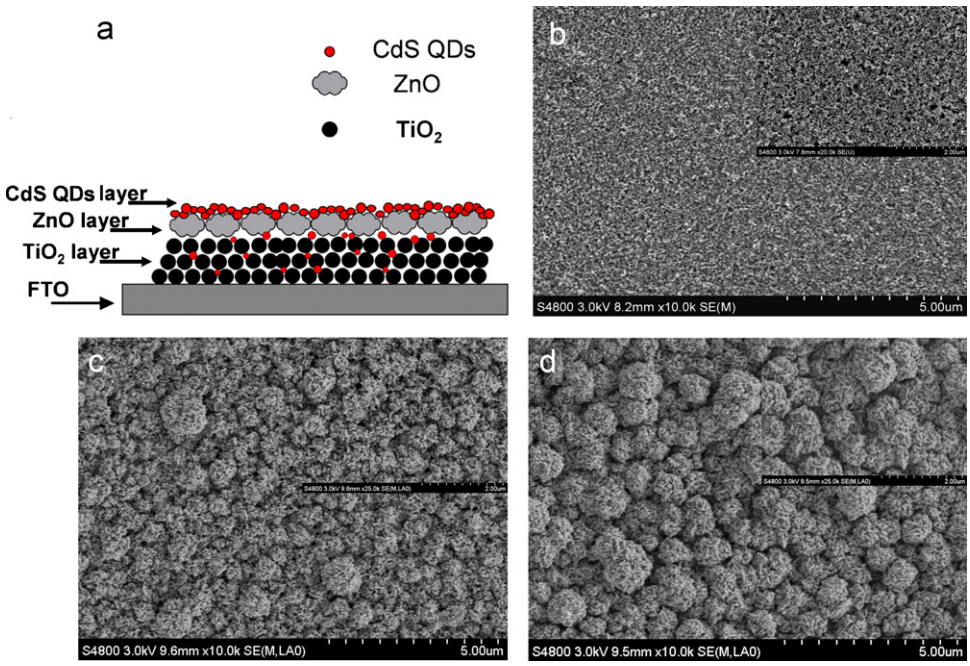

Fig. 1. (a) Schematic diagram of cascade structure of TiO_2/ZnO/CdS film; surface morphologies of (b) TiO_2, (c) TiO_2/ZnO and (d) TiO_2/ZnO/CdS films during the fabrication of cascade structure by FESEM measurements.

Despite the above progress, further exploration on photoanode is still necessary to carry out because there is still much scope to improve for above-mentioned DSSCs or QDSSCs in order to apply them in practice. It can be noticed that most of the reports employed various methods such as rf magnetron sputtering, chemical vapor deposition, sol–gel, electrochemical deposition or SILAR to deposit ZnO interlayer. But as a widely used, inexpensive, versatile, large-scale production technique, spray pyrolysis method is seldom studied by now to coat ZnO layer onto TiO_2 electrode for SSCs.

In this work, we reported CdS QDSSCs based on TiO_2/ZnO bilayer-structured film photoanode and polysulfide electrolyte. The ZnO layer was one-step synthesized and deposited on screen-printed TiO_2 layer by ultrasonic spray pyrolysis (USP) technology. A large improvement in the efficiency up to 1.56% is achieved as compared with 0.99% for the QDSSC based on the bare TiO_2 electrode. The formation of an inherent energy barrier between TiO_2 and CdS films and the passivation of surface traps on the TiO_2 film caused by the introduction of ZnO layer, which reduces the charge recombination and favors the electron transport, should be mainly responsible for the performance enhancement of TiO_2/ZnO/CdS cell.

2. Experimental

Fluorine-doped tin oxide (FTO) glass (resistivity: 14 Ω/□, Nippon Sheet Glass, Japan) was used as the substrate for nanocrystalline TiO_2 (P25, Degussa) electrodes. Zinc acetate dihydrate [$Zn(CH_3COO)_2{\cdot}2H_2O$], cadmium nitrate [$Cd(NO_3)_2$], sodium sulfide [$Na_2S$], methanol [$CH_3OH$], and Ethanol [$CH_3CH_2OH$] (analytical grade purity) were purchased from Shanghai Chemical Reagents Co. Ltd. and were used without further purification.

TiO_2 film was prepared by screen printing of TiO_2 paste on the FTO glass, followed by sintering at 500 °C for 30 min. The thicknesses of TiO_2 layer was about 5 μm. A precursor solution (0.15 M) was prepared by mixing $Zn(CH_3COO)_2{\cdot}2H_2O$ and distilled water. Then, the ZnO layer with the thickness of about 2 μm was deposited on the TiO_2 film from the precursor solution by USP (402AI) at a frequency of 1.65 MHz. The flow rate of air used as a carrier gas was 2 ml/min. The substrate of TiO_2 was kept at 430 °C for 1 h and the TiO_2/ZnO electrode was obtained.

CdS deposition on the TiO_2/ZnO film was performed by SILAR technique [34–36]. The film was dipped into an ethanol solution containing 0.5 M $Cd(NO_3)_2$ for 30 s, rinsed with ethanol, and then dipped for another 30 s into a 0.5 M Na_2S methanol solution and rinsed again with methanol. The two-step dipping procedure was considered to be 1 cycle. This sequential coating was repeated for 12 cycles [23,24]. Direct deposition of CdS on screen-printed TiO_2 (TiO_2/CdS) by SILAR process was carried out for comparison.

The morphology and structure of TiO_2, TiO_2/ZnO and CdS QDs incorporated TiO_2/ZnO (TiO_2/ZnO/CdS) electrodes were characterized by using a M21XVHF2Z (Mac Science Co. Ltd.) X-ray diffractometer with Cu Kα radiation (V = 35 kV, I = 20 mA), a Hatachi S-4800 field emission scanning electron microscope (FESEM), a JEOL-2010 high-resolution transmission electron microscope (HRTEM), respectively. The UV–vis absorption and transmittance spectra of TiO_2/CdS and TiO_2/ZnO/CdS films were detected using a UV–vis spectrophotometer (Hitachi U-3900).

The CdS QDSSCs were sealed in a sandwich structure with a 25 μm spacer (Surlyn) by using thin Au-sputtered FTO glass as counter electrode. Water/methanol (3:7 by volume) solution was used as a co-solvent of the polysulfide electrolyte [37]. The electrolyte solution consists of 0.5 M Na_2S, 2 M S and 0.2 M KCl. The active area of the cell was 0.25 cm^2. Photocurrent–voltage measurement was performed with a Keithley model 2440 Source Meter and a Newport solar simulator system (equipped with a 1 kW xenon arc lamp, Oriel) at one sun (AM 1.5 G, 100 mW cm^{-2}), which was calibrated with a reference Si reference solar cell (P/N 91150V, Oriel). Incident photon to current conversion efficiency (IPCE) was measured as a function of wavelength from 300 to 800 nm using an Oriel 300 W xenon arc lamp and a lock-in amplifier M 70104 (Oriel) under monochromator illumination. The electrochemical impedance spectroscopy (EIS) measurements were performed using an electrochemical workstation (AUTOLAB PGSTAT302N) under 100 mW cm^{-2} illumination in the frequency range of 0.1 Hz–100 kHz, and the applied bias voltage and ac amplitude were set at open-circuit voltage of the cells and 10 mV between the counter electrode and the working electrode, respectively.

3. Results and discussion

Fig. 1a depicts the schematic diagram of cascade structure of TiO_2/ZnO/CdS film in our experiment. The bilayer-structured TiO_2/ZnO film is formed on the FTO substrate and employed as the photoanode. The cascade structure of TiO_2/ZnO/CdS film is obtained when CdS QDs cover the ZnO layer by SILAR process with 12 cycles. Fig. 1b–d shows FESEM images (top views) of TiO_2, TiO_2/ZnO and TiO_2/ZnO/CdS films during the fabrication of cascade structure, respectively. The TiO_2 under layer film is constructed by the random agglomeration of tiny sized TiO_2 nanocrystalline particles. The deposition of micrometer-sized aggregates consisting of nanosized crystalline ZnO film forms more porous structures in TiO_2/ZnO bilayer, which favors the easy penetration of electrolyte, CdS adsorption and light scattering. When CdS is deposited onto TiO_2/ZnO film, an apparent difference in the surface morphology is

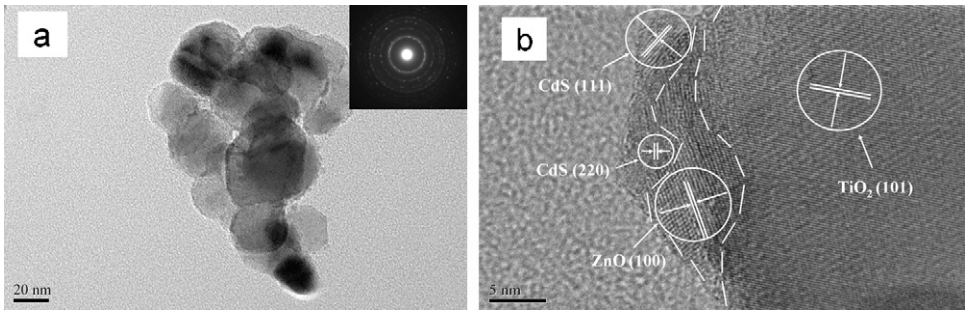

Fig. 2. (a) Low-magnification and (b) high-magnification HRTEM images of TiO_2/ZnO/CdS film. Inset is SAED pattern.

observed. This result indicates that a great amount of CdS QDs is assembled on the surface of TiO_2/ZnO film.

Fig. 2a shows a low-magnification HRTEM image of TiO_2/ZnO/CdS film. The larger size of the nanoparticles (about 40 nm) as compared with pure P25 TiO_2 particles (about 25 nm) indicating the surface of TiO_2 is coated with ZnO and CdS by USP and SILAR processes. The corresponding selected area electron diffraction (SAED) pattern in an upper right inset in Fig. 2a indicates that the TiO_2/ZnO/CdS film is a polycrystalline structure. Fig. 2b shows a high-magnification HRTEM image of the interface region in TiO_2/ZnO/CdS film. The larger crystallite is identified to be TiO_2 nanoparticle. The lattice spacing measured for this crystalline plane is 0.352 nm, corresponding to the (1 0 1) plane of anatase TiO_2. Around the TiO_2 crystallite, fine crystallites with various orientations and lattice spacing are observed. By carefully measuring and comparing the lattice parameters with the data in JCPD, the crystallites connecting to the TiO_2 have lattice fringes of 0.281 nm which is ascribed to (1 0 0) plane of ZnO. CdS with lattice spacing of 0.335 nm and 0.205 nm corresponding to (1 1 1) and (2 2 0) planes locates next to ZnO layer. Therefore, the cascade structure of TiO_2/ZnO/CdS film is confirmed by the HRTEM image.

Fig. 3 shows the X-ray diffraction (XRD) patterns of TiO_2, TiO_2/ZnO and TiO_2/ZnO/CdS films. The several peaks in curve for TiO_2 film correspond to (1 0 1), (1 0 3), (2 0 0), (1 0 5), (2 1 1) and (1 1 6) planes of nanocrystalline TiO_2 (JCPDS 21-1272). After ZnO is deposited on TiO_2 film, new peaks corresponding to (1 0 0), (0 0 2), (1 0 1), (1 0 2), (1 1 0), (1 0 3) and (1 1 2) planes of wurtzite hexagonal-shaped ZnO (JCPDS 36-1451) appear. The TiO_2/ZnO/CdS film exhibits a new weak peak corresponding to (1 1 1) plane of CdS [38], indicating the presence of CdS (JCPDS 80-0019).

The UV–vis absorption spectra of TiO_2/CdS and TiO_2/ZnO/CdS films are displayed in Fig. 4. The much higher absorbance of TiO_2/ZnO/CdS film at long wavelength range should be ascribed to enhanced light scattering due to the rougher surface after insertion of ZnO interlayer. Such an enhanced light scattering will be beneficial to efficiency improvement [39] and can be confirmed by the transmission spectra of the TiO_2/CdS and TiO_2/ZnO/CdS films in the inset of Fig. 4 because the long wavelength loss of transmission is mainly due to light scattering. The absorption edges, derived from the intersection of the sharply decreasing region of a spectrum [40], are ca. 520 nm for TiO_2/CdS and 540 nm for TiO_2/ZnO/CdS films, respectively. The band gaps of CdS obtained from the absorption edge are about 2.38 eV and 2.30 eV for TiO_2/CdS and TiO_2/ZnO/CdS films, respectively, which are larger than that of bulk CdS (2.25 eV) [41]. The small red-shift in the band gap of CdS in TiO_2/ZnO/CdS cell as compared with the one in TiO_2/CdS cell is possibly due to small size increase of deposited CdS QDs when ZnO layer is introduced on the surface of the TiO_2 film.

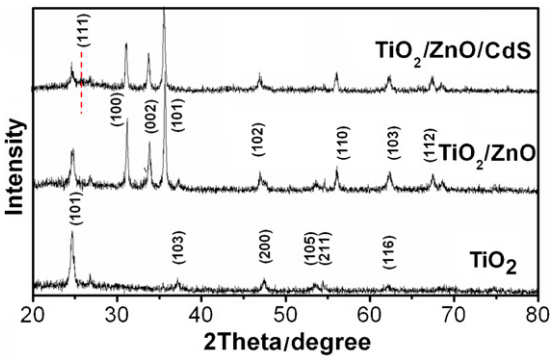

Fig. 3. XRD patterns of TiO_2, TiO_2/ZnO and TiO_2/ZnO/CdS films.

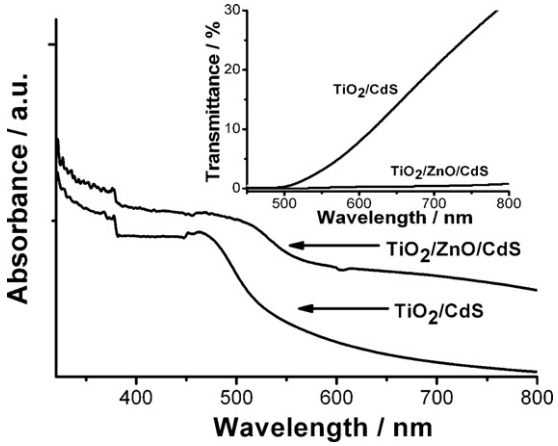

Fig. 4. UV–vis absorption spectra of TiO_2/CdS and TiO_2/ZnO/CdS films, and the inset is UV–vis transmission spectra of TiO_2/CdS and TiO_2/ZnO/CdS films.

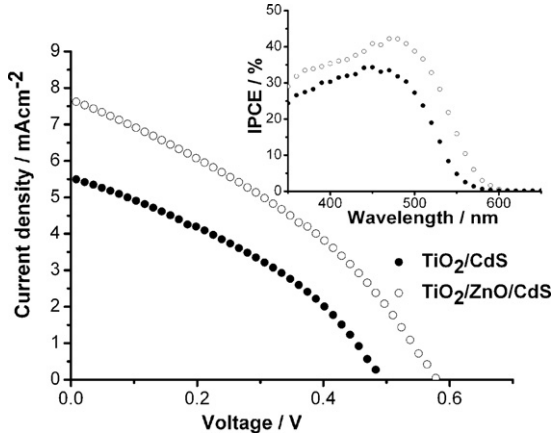

Fig. 5. *I–V* curves of TiO_2/CdS and TiO_2/ZnO/CdS cells. The inset is IPCE curves of TiO_2/CdS and TiO_2/ZnO/CdS cells.

Table 1
Photovoltaic parameters of TiO_2/CdS and TiO_2/ZnO/CdS cells.

Electrode	η/%	FF	V_{oc}/V	I_{sc}/mA cm^{-2}
TiO_2/CdS	0.99	0.36	0.49	5.52
TiO_2/ZnO/CdS	1.56	0.35	0.58	7.66

Fig. 5shows the *I–V* curves of TiO_2/CdS and TiO_2/ZnO/CdS cells. The open circuit potential (V_{oc}), short circuit current (I_{sc}), fill factor (FF) and conversion efficiency (η) of TiO_2/CdS and TiO_2/ZnO/CdS cells are listed in Table 1. It can be observed that the I_{sc}, V_{oc} and η have remarkably enhanced from 5.52 mA cm^{-2}, 0.49 V and 0.99% for TiO_2/CdS cell to 7.66 mA cm^{-2}, 0.58 V and 1.56% for TiO_2/ZnO/CdS cell. The improvement of I_{sc} and V_{oc} are caused by the formation of an inherent barrier layer at the TiO_2/CdS interface [28–31] and the passivation of the surface traps on the TiO_2 film by ZnO coating [30–32], which reduces the charge recombination and favors the electron transport.

If we assume that the conduction band of ZnO lies slightly above that of TiO_2, another possible mechanism responsible for the performance enhancement is the stepwise structure of band-edge levels constructed in the TiO_2/ZnO/CdS electrode. Similar structures of TiO_2/CdS/CdSe and TiO_2/ZnO/CdSe have been described by Refs. [6,33]. According to the data reported on the conduction and valence bands of TiO_2 (−4.2 eV and −7.4 eV), ZnO (−4.0 eV and −6.8 eV) [26] and CdS (−3.98 eV and −6.23 eV) [6,41], both the conduction and valence band edges of the three materials follow the order: TiO_2 < ZnO < CdS. Such a stepwise band-edge structure built in the TiO_2/ZnO/CdS electrode is also advantageous to the electron injection and hole recovery of the system [26,29,33].

From IPCE curves of TiO_2/CdS and TiO_2/ZnO/CdS cells in the inset of Fig. 5, TiO_2/ZnO/CdS cell achieve an IPCE value of maximum 43% at 475 nm while the one for TiO_2/CdS cell is only about 35% at 450 nm. The red-shift in the IPCE spectrum of TiO_2/ZnO/CdS cell as compared with the one of TiO_2/CdS cell should be due to the strong light scattering [42] and lower band gap of CdS after ZnO coating. The result indicates that ZnO coating really facilitate the excited electron transport from CdS to TiO_2 film [28,32].

The impedance spectra of TiO_2/CdS and TiO_2/ZnO/CdS cells are illustrated in Fig. 6. Two semicircles, including a small one at high frequency and a large one at low frequency, are observed in the Nyquist plots of EIS spectra and their corresponding equivalent circuit is shown in the inset of Fig. 6 [43,44]. R_s is the ohmic series resistance of FTO layer, Au layer and electrolyte. The small semicircle at high frequency is associated with the heterogeneous electron transfer at counter electrode/electrolyte interface and consists of charge transfer resistance (R_{ct}) and double layer capacitance

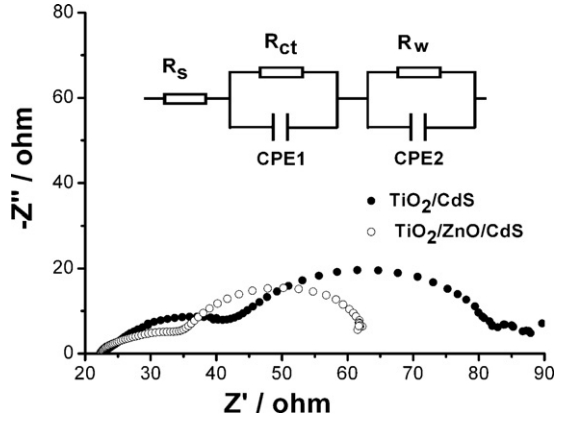

Fig. 6. EIS of TiO_2/CdS and TiO_2/ZnO/CdS cells. Inset is corresponding equivalent circuit.

(CPE1). The larger arc appearing at low frequency is due to the contribution from electron transport resistance (R_w) and interfacial capacitance (CPE2) at metal oxide semiconductor/CdS/electrolyte interface. The fitted R_w of the cell with TiO_2/ZnO/CdS electrode is about 32 Ω, much lower than that of the cell with TiO_2/CdS electrode (about 50 Ω), reflecting acceleration of electron transfer process in film photoanode. This result further confirms that the introduction of ZnO layer into TiO_2/CdS film favors the electron transfer from CdS to TiO_2.

4. Conclusion

The cascade structure of TiO_2/ZnO/CdS film was fabricated by combining screen printing, USP and SILAR processes to improve the photovoltaic performance of QDSSCs. The structure, morphology and impedance of TiO_2/ZnO electrode and the photovoltaic performance of TiO_2/ZnO/CdS cell were investigated. The results show that the η of TiO_2/ZnO/CdS cell reaches up to 1.56% under one sun illumination, which is 57% higher than that of TiO_2/CdS cell. Such an enhancement in photovoltaic performance should be mainly the ascribed to the formation of an inherent barrier layer at the TiO_2/CdS interface and the passivation of the surface traps on the TiO_2 film by ZnO coating, which reduces the charge recombination and favors the electron transport.

Acknowledgement

This work was supported by Special Project for Nanotechnology of Shanghai (No. 1052nm02700).

References

[1] B. O'Regan, M. Grätzel, Nature 353 (1991) 737.
[2] S.K. Sharma, A.I. Inamdar, H. Im, B.G. Kim, P.S. Patil, J. Alloys Compd. 509 (2011) 2.
[3] J.X. Mou, W.G. Zhang, J. Fan, H. Deng, W. Chen, J. Alloys Compd. 509 (2011) 961.
[4] I. Mora-Sero, S. Gimenez, F. Fabregat-Santiago, R. Gomez, Q. Shen, T. Toyoda, J. Bisquert, Acc. Chem. Res. 42 (2009) 1848.
[5] A. Qurashi, M.F. Hossain, M. Faiz, N. Tabet, M.W. Alam, N.K. Reddy, J. Alloys Compd. 503 (2010) L40.
[6] Y.L. Lee, Y.S. Lo, Adv. Funct. Mater. 19 (2009) 604.
[7] P. Sudhagar, J.H. Jung, S. Park, R. Sathyamoorthy, H. Ahn, Y.S. Kang, Electrochim. Acta 55 (2009) 113.
[8] E.M. Barea, M. Shalom, S. Gimenez, I. Hod, I. Mora-Sero, A. Zaban, J. Bisquert, J. Am. Chem. Soc. 132 (2010) 6834.
[9] O. Niitsoo, S.K. Sarkar, C. Pejoux, S. Ruhle, D. Cahen, G. Hodes, J. Photochem. Photobiol. A 181 (2006) 306.
[10] W. Lee, J. Lee, S. Lee, W. Yi, S.H. Han, B.W. Cho, Appl. Phys. Lett. 92 (2008) 153510.
[11] G. Zhu, T. Lv, L.K. Pan, Z. Sun, C.Q. Sun, J. Alloys Compd. 509 (2011) 362.
[12] J.M. Jang, C.R. Kim, H. Ryu, M. Razeghi, W.G. Jung, J. Alloys Compd. 463 (2008) 503.
[13] J. Chen, D.W. Zhao, J.L. Song, X.W. Sun, W.Q. Deng, X.W. Liu, W. Lei, Electrochem. Commun. 11 (2009) 2265.
[14] S.Q. Fan, D. Kim, J.J. Kim, D.W. Jung, S.O. Kang, J. Ko, Electrochem. Commun. 11 (2009) 1337.
[15] L.J. Diguna, Q. Shen, J. Kobayashi, T. Toyoda, Appl. Phys. Lett. 91 (2007) 023116.
[16] J. Mou, W. Zhang, J. Fan, H. Deng, W. Chen, J. Alloys Compd. 509 (2011) 961.
[17] C.M. Chen, Y.C. Hsu, S.J. Cherng, J. Alloys Compd. 509 (2011) 872.
[18] H. Yu, S.Q. Zhang, H.J. Zhao, B.F. Xue, P.R. Liu, G. Will, J. Chem. Phys. C 113 (2009) 16277.
[19] G. Zhu, Z.J. Cheng, T. Lv, L.K. Pan, Q.F. Zhao, Z. Sun, Nanoscale 2 (2010) 1229.
[20] M.D. Wei, K.X. Wang, M. Yanagida, H. Sugihara, M.A. Morris, J.D. Holmes, H.S. Zhou, J. Mater. Chem. 17 (2007) 3888.
[21] S.F. Wang, K.K. Rao, C.K. Yang Thomas, H.P. Wang, J. Alloys Compd. 509 (2011) 1969.
[22] A. Braga, S. Gimenez, I. Concina, A. Vomiero, I. Mora-Sero, J. Phys. Chem. Lett. 2 (2011) 454.
[23] G. Zhu, T. Xu, T. Lv, L.K. Pan, Q.F. Zhao, Z. Sun, J. Electroanal. Chem. 650 (2011) 248.
[24] G. Zhu, F.F. Su, T. Lv, L.K. Pan, Z. Sun, Nanoscale Res. Lett. 5 (2010) 1749.
[25] Y.Q. Wang, Y.M. Sun, K. Li, Mater. Lett. 63 (2009) 1102.
[26] S.J. Roh, R.S. Mane, S.K. Min, W.J. Lee, C.D. Lokhande, S.H. Han, Appl. Phys. Lett. 89 (2006) 253512.
[27] S. Wu, H. Han, Q. Tai, J. Zhang, B.L. Chen, S. Xu, C. Zhou, Y. Yang, H. Hu, X.Z. Zhao, Appl. Phys. Lett. 92 (2008) 122106.
[28] M.C. Kao, H.Z. Chen, S.L. Young, Appl. Phys. A 97 (2009) 469.

[29] S.S. Kim, J.H. Yum, Y.E. Sung, Sol. Energy Mater. Sol. Cells 79 (2003) 495.
[30] K.E. Kim, S.R. Jang, J. Park, R. Vittal, K.J. Kim, Sol. Energy Mater. Sol. Cells 91 (2007) 366.
[31] S.H. Kang, J.Y. Kim, Y. Kim, H.S. Kim, Y.E. Sung, J. Phys. Chem. C 111 (2007) 9614.
[32] Z.S. Wang, C.H. Huang, Y.Y. Huang, Y.J. Hou, P.H. Xie, B.W. Zhang, H.M. Cheng, Chem. Mater. 13 (2001) 678.
[33] W. Lee, S.H. Kang, J.Y. Kim, G.B. Kolekar, Y.E. Sungand, S.H. Han, Nanotechnology 20 (2009) 335706.
[34] D.R. Baker, P.V. Kamat, Adv. Funct. Mater. 19 (2009) 805.
[35] H.J. Lee, H.C. Leventis, S.J. Moon, P. Chen, S. Ito, S.A. Haque, T. Torres, F. Nuesch, T. Geiger, S.M. Zakeeruddin, M. Grätzel, M.K. Nazeeruddin, Adv. Funct. Mater. 19 (2009) 2735.
[36] Y.J. Tak, S.J. Hong, J.S. Lee, K.J. Yong, J. Mater. Chem. 19 (2009) 5945.
[37] Y.L. Lee, C.H. Chang, J. Power Sources 185 (2008) 584.
[38] B.A. Gregg, F. Pichot, S. Ferrere, C.L. Fields, J. Phys. Chem. B 105 (2001) 1422.
[39] Y.Z. Zheng, X. Tao, L.X. Wang, H. Xu, Q. Hou, W.L. Zhou, J.F. Chen, Chem. Mater. 22 (2010) 928.
[40] S. Banerjee, S.K. Mohapatra, P.P. Das, M. Misra, Chem. Mater. 20 (2008) 6784.
[41] M. Grätzel, Nature 414 (2001) 338.
[42] W. Chen, Y.C. Qiu, Y.C. Zhong, K.S. Wong, S.H. Yang, J. Phys. Chem. A 114 (2010) 3127.
[43] N. Yang, J. Zhai, D. Wang, Y. Chen, L. Jiang, ACS Nano 4 (2010) 887.
[44] Q. Wang, J.E. Moser, M. Grätzel, J. Phys. Chem. B 109 (2005) 14945.